Available online at www.sciencedirect.com

SciVerse ScienceDirect

Ceramics International 38 (2012) 4669–4675

CERAMICS INTERNATIONAL

www.elsevier.com/locate/ceramint

$Ce_{0.9}Gd_{0.1}O_{1.95}$ supported $La_{0.6}Sr_{0.4}Co_{0.2}Fe_{0.8}O_{3-\delta}$ cathodes for solid oxide fuel cells

Ju Hee Kim, Haekyoung Kim *

School of Materials Science & Engineering, Yeungnam University, Gyeongsan 712-749, Republic of Korea

Received 6 January 2012; received in revised form 15 February 2012; accepted 15 February 2012
Available online 23 February 2012

Abstract

Lanthanum-based iron- and cobalt-containing perovskite has a high potential as a cathode material because of its high electro-catalytic activity at a relatively low operating temperature in solid oxide fuel cells (SOFCs) (600–800). To enhance the electro-catalytic reduction of oxidants on $La_{0.6}Sr_{0.4}Co_{0.2}Fe_{0.8}O_{3-\delta}$ (LSCF), Ga doped ceria ($Ce_{0.9}Gd_{0.1}O_{1.95}$, GDC) supported LSCF (15LSCF/GDC) is successfully fabricated using an impregnation method with a ratio of 15 wt% LSCF and 85 wt% GDC. The cathodic polarization resistances of 15LSCF/GDC are 0.015 Ω cm^2, 0.03 Ω cm^2, 0.11 Ω cm^2, and 0.37 Ω cm^2 at 800 °C, 750 °C, 700 °C, and 650 °C, respectively. The simply mixed composite cathode with LSCF and GDC of the same compositions shows 0.05 Ω cm^2, 0.2 Ω cm^2, 0.56 Ω cm^2, and 1.20 Ω cm^2 at 800 °C, 750 °C, 700 °C, and 650 °C, respectively. The fuel cell performance of the SOFC with 15LSCF/GDC shows maximum power densities of 1.45 W cm^{-2}, 1.2 W cm^{-2}, and 0.8 W cm^{-2} at 780 °C, 730 °C, and 680 °C, respectively. GDC supported LSCF (15LSCF/GDC) shows a higher fuel cell performance with small compositions of LSCF due to the extension of triple phase boundaries and effective building of an electronic path.

Keywords: Solid oxide fuel cell; Cathodes; Anode supported cell; Mixed ionic electronic conductor; Supported cathode

1. Introduction

Solid oxide fuel cells (SOFCs) are believed to be the most promising future component of energy generation for power plants and distributed power systems. To operate at intermediate temperatures (600–800 °C), perovskite-based compounds having the general formula of $La_{0.6}Sr_{0.4}Co_{0.2}Fe_{0.8}O_{3-\delta}$ (LSCF) have been reported to be very effective owing to their high catalytic activity with a Gd-doped ceria (GDC)-based interlayer [1–6]. However, with a high activation enthalpy for oxygen self-diffusion in LSCF [7], the ionic conductivity of a LSCF cathode drops rapidly as the temperature decreases. To enhance the ionic conductivity of the cathode electrode and prevent the coarsening of the cathode, the addition of a second phase such as GDC has been reported [8–14]. It has been confirmed that the formation of a composite cathode can beneficially reduce the polarization resistance of a pure LSCF cathode; this performance is related to the sintering temperature, microstructure (such as the grain size and porosity), and the composition of the LSCF and the GDC [3,7,15,16]. Electrochemical reactions in composite cathodes of LSCF and GDC occur at the triple phase boundary (LSCF, GDC, and oxygen gas) as well as at the surface of LSCF. The electrochemical performance of a LSCF-type cathode can also be varied by processing and micro-structural parameters of the cathode materials [15–18]. Small-particle-size and high-surface area in nanocrystalline materials are favored for the cathode electrode for SOFCs, which results in enhancement of an electro-catalytic reduction of oxidant along with a higher catalytic activity [15–22]. The composite cathodes can be prepared by a simple micro-scale mixture of LSCF and GDC. To extend the triple phase boundary, nano-scaled heterogeneous powders in the form of either a surface coated or core–shell structure have been also reported for a composite cathode in SOFCs for better long-term stability and high-performance [23–26].

In this study, GDC supported LSCF was prepared with a LSCF complex solution and GDC particles. The surface of the GDC was coated and dried several times with LSCF complex solutions for impregnations of 15 wt% LSCF on GDC. Paste

* Corresponding author. Tel.: +82 53 810 2536; fax: +82 53 810 4628.
E-mail address: hkkim@ynu.ac.kr (H. Kim).

0272-8842/$36.00
doi:10.1016/j.ceramint.2012.02.049

with GDC supported LSCF was printed and sintered onto Ni–YSZ support/Ni–YSZ functional layer/YSZ electrolyte/GDC interlayer anode-supported SOFCs. The cathode with GDC supported LSCF and the simply mixed composite cathode of GDC and LSCF were characterized in terms of cathode polarization and fuel cell performances as a function of temperatures and compositions.

2. Experimental procedure

The LSCF complex solution was prepared with nitrate salts of La^{3+}, Sr^{2+}, Co^{3+}, and Fe^{3+}. The complex method with chelating agent is described below. Lanthanum nitrate, strontium nitrate, cobalt nitrate, and ferric nitrate were dissolved at a molar ratio of 3:2:1:4 in deionized water to prepare a homogeneous metal nitrate solution. The solid citric acid and ethylenediaminetetraacetic acid (EDTA) powder as chelating agents were added to the mixed metal nitrate solution and then the solution was heated in a water bath at 70 °C. Nitrate forms of metal precursors, all in analytical grades, were used as metal sources. EDTA powder and crystallized citric acid were used as the raw materials for chelation, which both have purities higher than 99.5%.

GDC of 5 $m^2\ g^{-1}$ was purchased from ANNA Kasei as a support for GDC supported LSCF. The surfaces of GDC powders were impregnated with a concentrated LSCF complex solution, 0.6 M of metal nitrate, and dried at 150 °C. Impregnation and drying step was repeated 3–4 times. After impregnation of a ratio 15 wt% LSCF to GDC, GDC supported LSCF (15LSCF/GDC) was calcined at 700 °C for 3 h. The simply mixed composite cathodes (SMC) of GDC and LSCF were prepared with LSCF and GDC with a ratio of 15:85 wt%, 30:70 wt%, 40:70 wt%, 50:50 wt%, 60:40 wt%, 70:30 wt%, and 100:0 wt% by using a three roll mill. The SMCs are coded with the composition of LSCF. LSCF powder for simply mixed composite cathodes was prepared from complex solutions. The LSCF complex solution was heated to evaporate water and dried in a vacuum oven of 120 °C. After drying, the powder was calcined at 700 °C for 3 h. The synthesized powders were characterized with X-ray diffractometer (XRD) and scanning electron microscopy (SEM).

The GDC supported LSCF cathode and simply mixed composite cathodes were characterized with electrolyte-supported symmetric cathode |YSZ| cathode cells. The cathode paste was prepared by mixing cathode materials with organic binder (ethyl cellulose, di-ethylene glycol butyl ether, and α-terpinol) in ratio of 50:50 wt%. The symmetric cells were prepared by screen-printing and sintering cathodes pastes on both sides of the YSZ electrolyte. The impedance spectra were obtained in the frequency range of 100 kHz–0.1 Hz with applied AC voltage amplitude of 100 mV at the temperature range of 580–780 °C. The cathodic polarization resistances were determined from the differences between high- and low-frequency intercepts on the impedance spectra and divided by two.

To characterize the fuel cell performance of the SOFCs, the GDC supported LSCF was mixed with organic binder, ethyl cellulose, and di-ethylene glycol butyl ether with α-terpinol. The Ni–YSZ/YSZ/GDC anode-supported cells were cut into 1 in diameter circles from a 25 cm × 25 cm plate prepared by tape-casting and a co-fired method. The cathode paste was printed on the Ni–YSZ/YSZ/GDC anode-supported cell and sintered at 900 °C for 4 h. The active cathode area was 0.785 cm^2. The cathode polarizations of 15LSCF/GDC and 15LSCF SMC cathode were measured with an impedance analyzer. Impedance spectra were collected in an open-circuit condition in the frequency range of 100 kHz–0.1 Hz (perturbation voltage: 100 mV). The fuel cell performances were tested with a 300 $cm^3\ min^{-1}$ of 97% H_2–3% H_2O and 1000 $cm^3\ min^{-1}$ of air.

3. Results and discussion

The schematic diagrams of GDC supported LSCF are shown in Fig. 1. The LSCF complex solution was impregnated and dried on the surface of GDC several times for impregnation of 15 wt% of LSCF to GDC. The triple phase boundaries are expected to be built with a small amount of LSCF. The GDC supported LSCF powders (15LSCF/GDC) are investigated with TEM images and XRD. As shown in Fig. 2, the XRD patterns of LSCF and GDC are observed in 15LSCF/GDC, respectively. It is also confirmed by TEM-EDS analysis that particles less than

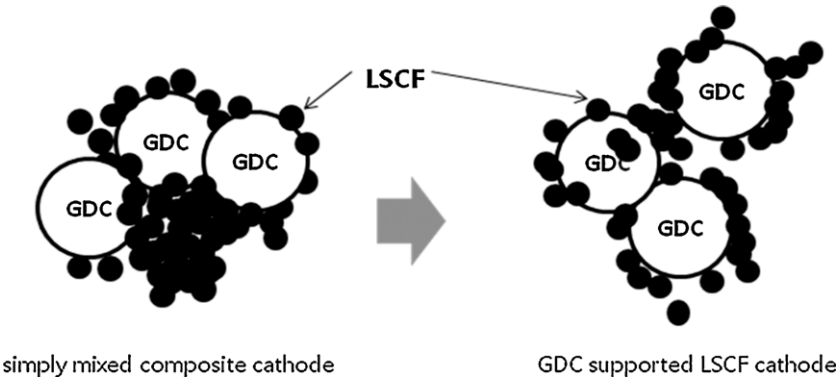

Fig. 1. Schematic diagram of LSCF–GDC composite and GDC supported LSCF.

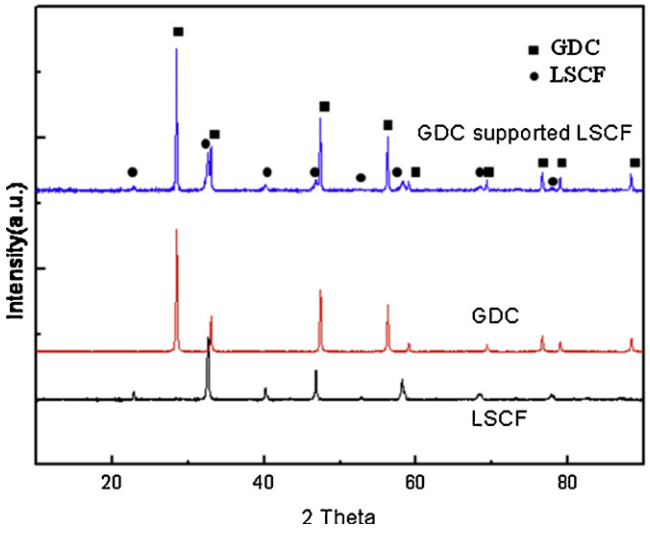

Fig. 2. XRD patterns of GDC supported LSCF.

20 nm are impregnated on the surface of the GDC powder as shown in Fig. 3. The 15LSCF/GDC can be divided into two different regions: GDC regions (darker area) and LSCF regions (brighter area). Detailed composition profiles obtained from selected areas in the TEM image are shown in Fig. 3(a). The GDC spectra in 1, 4, 5, and 7 positions and the LSCF spectra in 2, 3, and 6 positions are observed in Fig. 3(a). The compositional mapping detected by EDS shows the LSCF is homogeneously impregnated on the surface of GDC as shown in Fig. 3(b). The La elements are distributed uniformly on the surface of particles, while the Ce elements are located in the dark middle region. EDS compositional mapping clearly confirms that the GDC supported LSCF is successfully prepared via impregnation methods. In the form of core–shell structure or infiltrated structure, it is not easy to classify the distinct difference in two regions in the heterogeneous powder [25,27]. However, the GDC supported LSCF via an impregnation method can be classified into two distinguishable regions of GDC and LSCF as shown in Fig. 3(a). The LSCF coated on the GDC surface may extend the triple phase boundaries and be expected to show higher fuel cell performances with a small amount.

The cathode of 20–30 μm is printed on both sides of YSZ in the electrolyte-supported symmetric cathode/YSZ/cathode cells as shown in Fig. 4. The impedances of the symmetric cells with 15LSCF/GDC (GDC supported LSCF cathode) and 15LSCF SMC cathode are characterized as a function of temperature as shown in Fig. 5. The cathodic polarization resistances were determined from the differences between high- and low-frequency intercepts on the impedance spectra and divided by 2. The cathodic polarization resistances (R_p) of GDC supported LSCF are 0.015 Ω cm^2, 0.03 Ω cm^2, 0.11 Ω cm^2, 0.35 Ω cm^2, and 0.68 Ω cm^2 at 780 °C, 730 °C, 680 °C, 630 °C and 580 °C, respectively. The R_p of 15LSCF SMC are 0.065 Ω cm^2, 0.21 Ω cm^2, 0.57 Ω cm^2, and 1.13 Ω cm^2 at 780 °C, 730 °C, 680 °C, and 630 °C, respectively. The cathodic polarization resistances of GDC supported LSCF cathode show 3–5 times lower than those of the 15LSCF SMC cathode. To investigate the effect of the impregnation method, SMC cathodes were characterized as a function of LSCF compositions. The cathodic polarization of GDC supported LSCF cathode and simply mixed composite cathodes are plotted as shown in Fig. 6. The 60LSCF SMC shows the lowest cathodic polarization resistance at all temperature ranges. These results can be compared with Leng's work [14]. In their work, the 40LSCF–60GDC composite cathode has the lowest polarization. The difference of LSCF and GDC in three phase boundaries may result in the different cathodic polarization. The cathodic polarization resistances (R_p) of cells are the lowest in 60LSCF SMC, which are 0.015 Ω cm^2 at 800 °C and 0.02 Ω cm^2 at 750 °C. The GDC supported LSCF shows polarization resistance of 0.015 Ω cm^2 at 800 °C and 0.035 Ω cm^2 at 750 °C. The cathodic polarization resistance of GDC supported LSCF shows values similar to 60LSCF SMC and higher than 50LSCF SMC. The GDC supported LSCF with a small amount of LSCF with 15 wt%, shows a higher performance than a simply mixed composite cathode with LSCF of 50 wt%. The triple phase boundaries for oxygen reduction reaction of LSCF, GDC and oxidants are extended with the nano-sized LSCF on GDC surface, which result in the lower cathodic polarization resistance. The nano-sized LSCF coated on GDC surface is very effective for building the electronic conducting path with a small amount of LSCF. It is confirmed that the morphology of a cathode is one of the important factors for improving fuel cell performance. These phenomena can be also be explained by an ambipolar resistivity model of a porous composite cathode developed by Dusastre and Kilner [1]. At a very high GDC content, 30LSCF and 15LSCF, the electron-conducting path may not be effectively built up, which results in a sharp increase in polarization resistance. In addition, the presence of a non-continuous electron-conducting phase in a 30LSCF and 15LSCF composite cathode leads to high ohmic resistance of the composite cathode and high contact resistance between the cathode and electrolyte. However, the GDC supported LSCF has the morphological effects for building the electronic conducting path with a small amount of LSCF of 15 wt%. To lower the polarization resistance, careful design and fabrication are needed to maximize the effects of the materials.

The plot of ln (R_p^{-1}) vs ($1000T^{-1}$) in Fig. 7(a) shows the activation energy for the oxygen reduction reaction of a GDC supported LSCF cathode and simply mixed cathodes. The activation energy of cathodes is shown as a function of a LSCF composition in Fig. 7(b). With increasing LSCF, the activation energy decrease and is the lowest in 60LSCF SMC of 136.6 kJ mol^{-1}. The GDC supported LSCF cathode shows an activation energy of 156.1 kJ mol^{-1}. The activation energy in 60LSCF and 50LSCF is similar and 15LSCF SMC show much higher activation energy. However, the GDC supported LSCF cathode has a lower activation energy than 15LSCF SMC and the impregnation method is also effective for lowering the activation energy with a small amount.

The SOFCs were prepared with GDC supported LSCF, 15LSCF SMC cathode and 50LSCF SMC. The cross-sectional image of an SOFC with a GDC supported LSCF is shown in

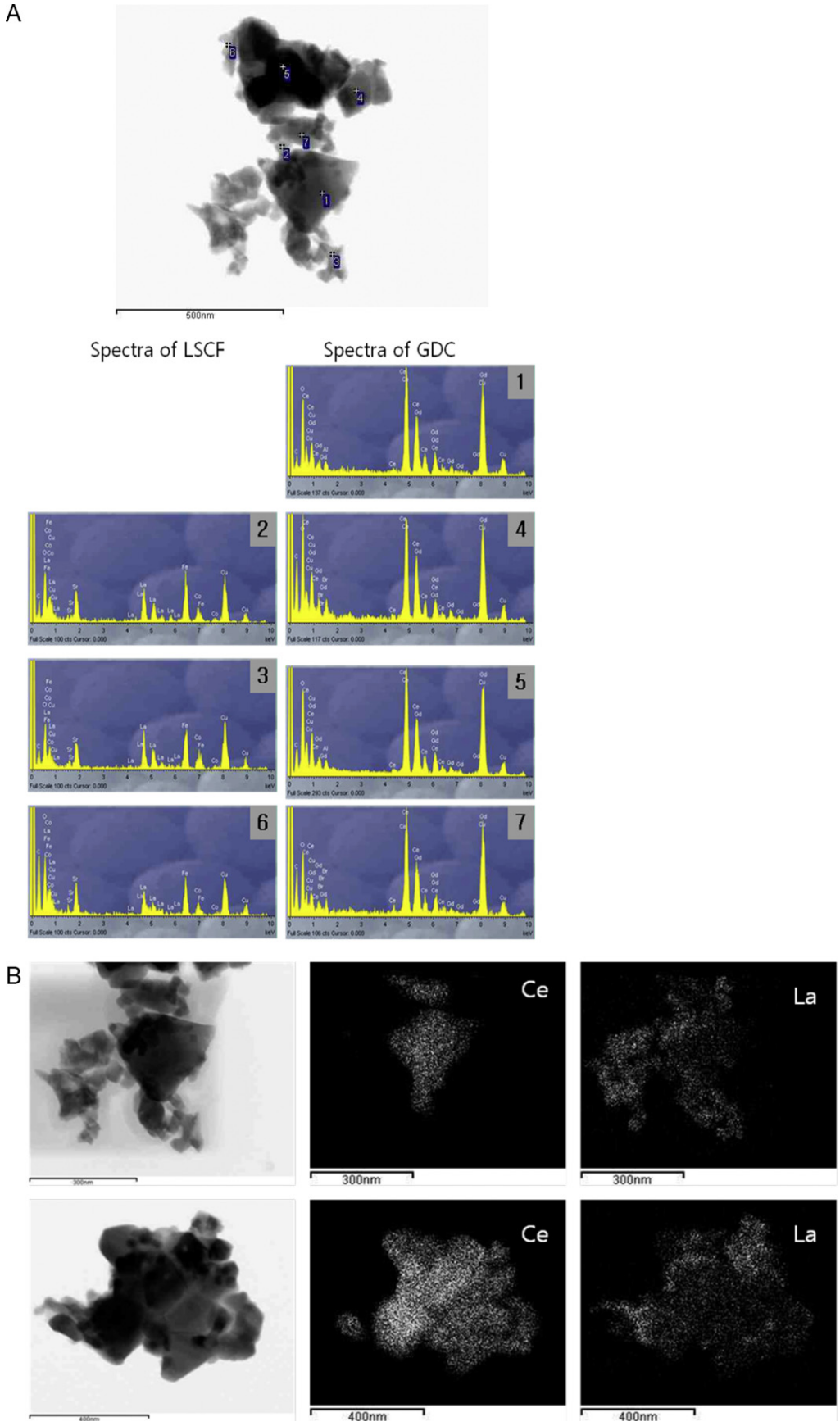

Fig. 3. (a) TEM-EDS spectra of the GDC supported LSCF, and (b) mapping of Ce and La elements of the GDC supported LSCF.

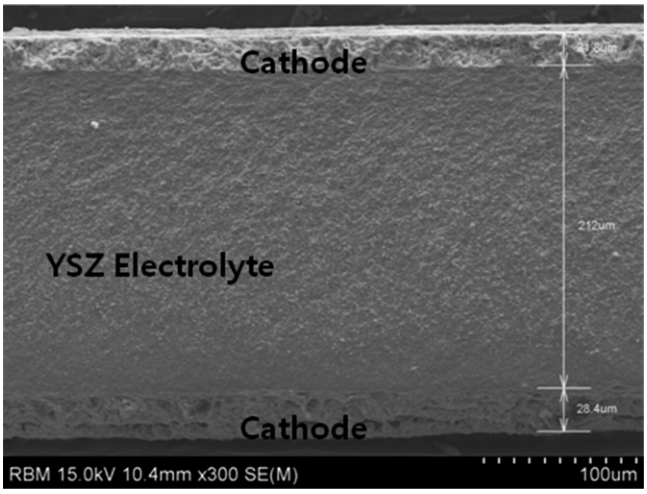

Fig. 4. Cross-sectional images of the electrolyte-supported symmetric cathode |YSZ| cathode cells.

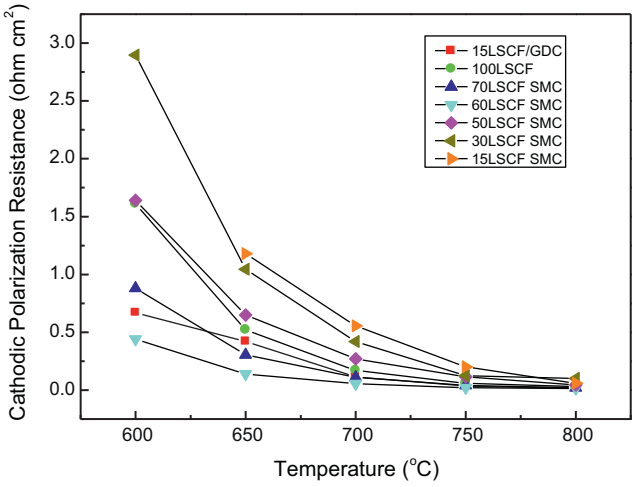

Fig. 6. Cathodic polarization resistances of the GDC supported LSCF and simply mixed composite cathodes.

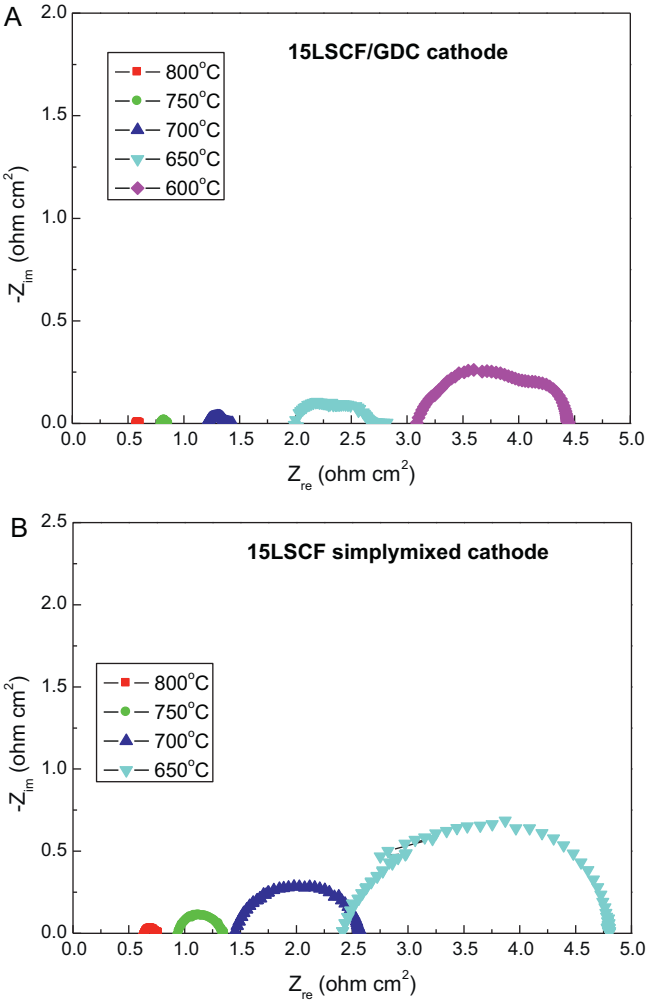

Fig. 5. (a) Impedance spectra of the GDC supported LSCF cathode (15LSCF/GDC) and (b) impedance spectra of 15LSCF simply mixed cathode (15LSCF SMC).

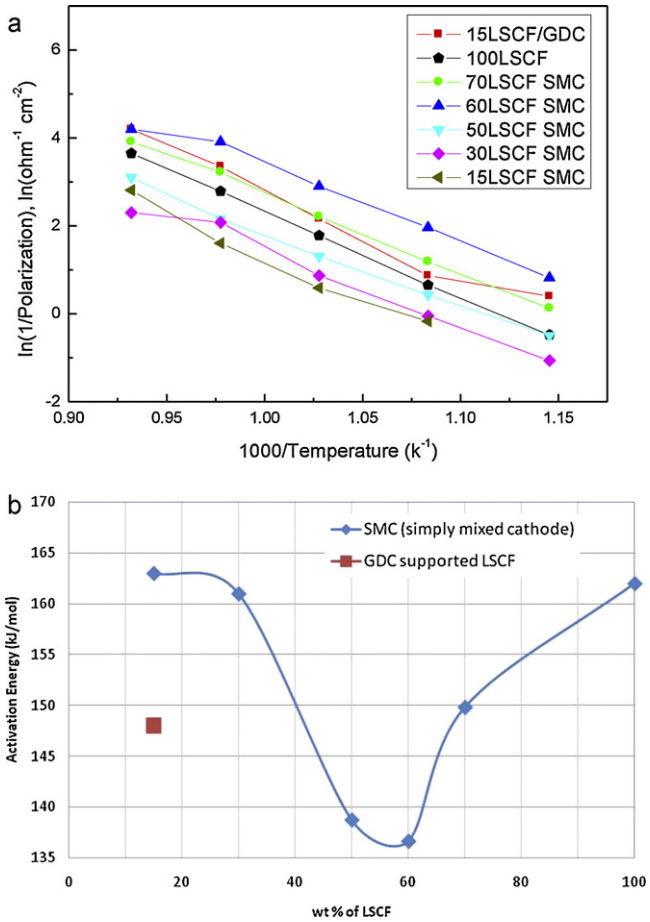

Fig. 7. (a) ln ($1/R_p$) vs 1000/temperature of the GDC supported LSCF and simply mixed composite cathode, and (b) activation energy with LSCF composition.

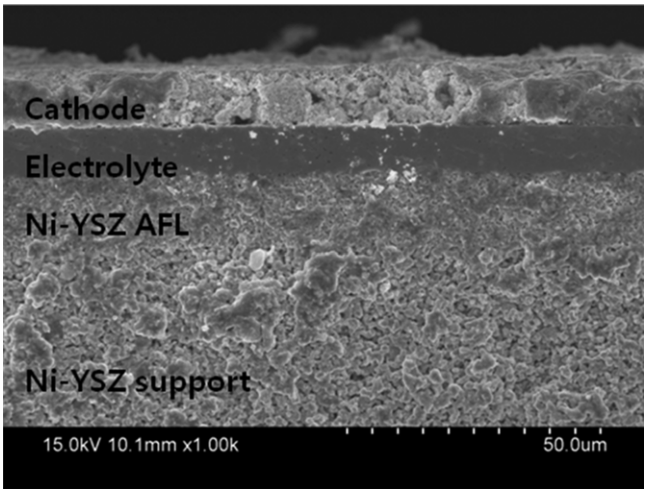

Fig. 8. Cross-sectional images of SOFCs with 15LSCF/GDC.

Fig. 8, which consists of GDC supported LSCF (−30 μm) as a cathode, GDC (−1 μm) as an interlayer, YSZ (−10 μm) as an electrolyte, Ni–YSZ (−20 μm) as an anode functional layer, and Ni–YSZ (−800 μm) as a support. Good adhesion is observed between the GDC interlayer and the GDC supported LSCF. The fuel cell performances of the SOFCs were characterized with H_2–H_2O of 300 cm^3 min^{-1} and air of 1000 cm^3 min^{-1}. The current–voltage curves are shown in Fig. 9. The SOFC with the GDC supported LSCF cathode at 0.8 V shows 1.17 A cm^{-2}, 0.92 A cm^{-2}, and 0.66 A cm^{-2}, at 780 °C, 730 °C, and 680 °C, respectively. The maximum powder density of the SOFC with a GDC supported LSCF cathode is over 1.5 W cm^{-2} at 780 °C. The SOFC with 50LSCF SMC at 0.8 V shows 0.72 A cm^{-2}, 0.48 A cm^{-2}, and 0.37 A cm^{-2} at 780 °C, 730 °C and 680 °C, respectively. The maximum powder density of the SOFC with 50LSCF SMC is 1.2 W cm^{-2} at 780 °C. The SOFC with 60LSCF SMC at 0.8 V shows 1.12 A cm^{-2}, 0.73 A cm^{-2}, and 0.52 A cm^{-2} at 780 °C, 730 °C and 680 °C, respectively. The SOFC with 15LSCF SMC shows the maximum powder densities of less than 0.2 W cm^{-2}. The 15 wt% of LSCF in 15LSCF/GDC may not be enough to build the electronic path for electrochemical reactions. The SOFC with GDC supported LSCF shows a higher fuel cell performance than the SOFC with 50LSCF SMC and a lower fuel cell performance than the SOFC with 60LSCF SMC and this is consistent with symmetric cell results. The 15LSCF SMC shows a poor fuel cell performance due to a deficient amount of LSCF for electronic conducting path. The heterogeneous powder of LSCF and GDC for the SOFC should be designed with consideration of building electrochemical reaction sites. The impregnated LSCF with nano sized morphologies is a very effective cathode for developing the ionic and electronic conducting path. The GDC supported LSCF is effective for building triple phase boundaries for electrochemical reactions with a smaller amount of LSCF.

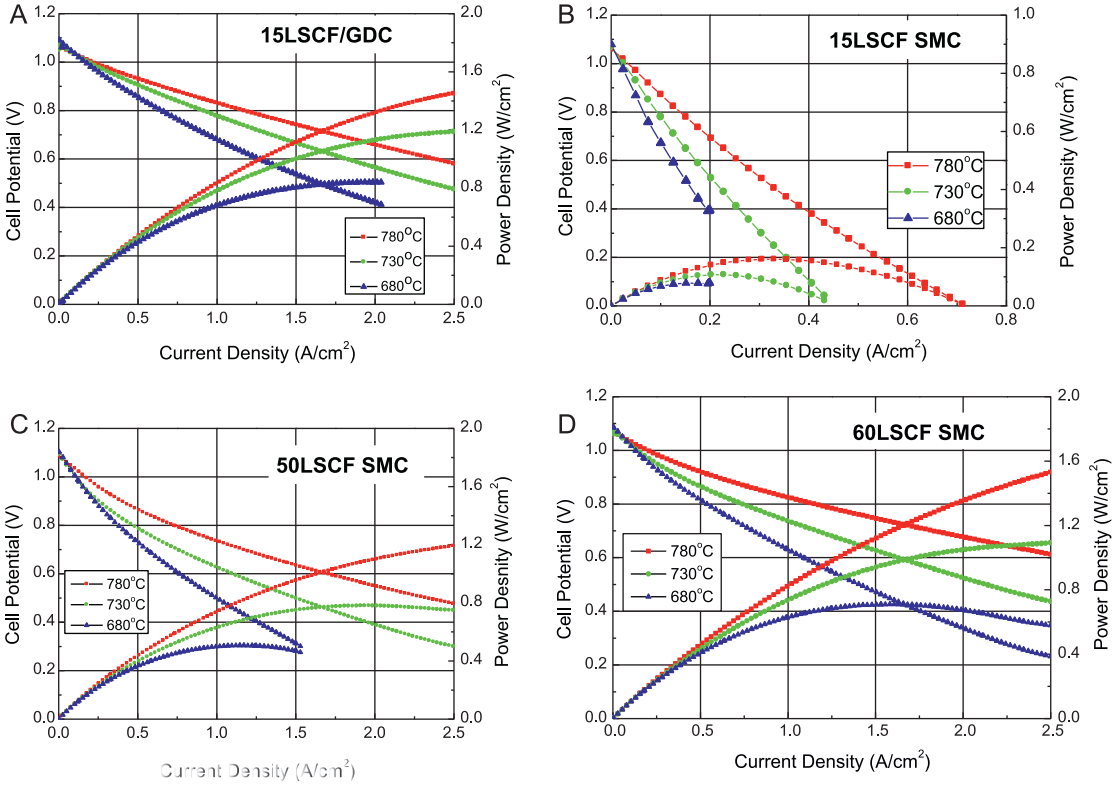

Fig. 9. Fuel cell performances: (a) SOFC with 15LSCF/GDC cathode, (b) SOFC with 15LSCF SMC, (c) SOFC with 50LSCF SMC, and (d) SOFC with 60LSCF SMC.

4. Conclusion

The GDC ($Ce_{0.9}Gd_{0.1}O_{1.95}$) supported LSCF ($La_{0.6}Sr_{0.4}Co_{0.2}Fe_{0.8}O_{3-\delta}$) with 15 wt% of LSCF was successfully synthesized by an impregnation method with LSCF complex solutions. The TEM-EDS analysis shows that LSCFs of less than 20 nm are impregnated on the GDC surface. The triple phase boundaries among LSCF, GDC and air are expected to be extended and results in higher fuel cell performances. The symmetric cell of cathode/YSZ/cathode shows the GDC supported LSCF has lower cathodic polarization than the 50LSCF SMC simply mixed composite cathode. The polarization resistances (R_p) of GDC supported LSCF are 0.015 $\Omega\,cm^2$, 0.03 $\Omega\,cm^2$, 0.11 $\Omega\,cm^2$, 0.35 $\Omega\,cm^2$, and 0.68 $\Omega\,cm^2$ at 800 °C, 750 °C, 700 °C, 650 °C and 600 °C, respectively. The cathodic polarization resistance of GDC supported LSCF is 3–5 times lower than that of 15LSCF SMC composite cathode. The smaller amount LSCF of 15 wt% in GDC supported LSCF may be effective for building an electronic path for an electrochemical reaction. The SOFC with the GDC supported LSCF cathode at 0.8 V shows 1.17 A cm^{-2}, 0.92 A cm^{-2}, 0.66 A cm^{-2}, and 0.38 A cm^{-2}at 780 °C, 730 °C, and 680 °C, respectively. The maximum powder density of the SOFC with the GDC supported LSCF cathode is over 1.5 W cm^{-2} at 780 °C. A morphological difference in the starting particles of GDC supported LSCF may result in lower cathodic polarization resistance and increase fuel cell performance.

Acknowledgment

This work was supported by the National Research Foundation (NRF) of Korea Grant funded by the Korean Government (MEST) (NRF-2011-0009667).

References

[1] V. Dusastre, J.A. Kilner, Optimisation of composite cathodes for intermediate temperature SOFC applications, Solid State Ionics 126 (1999) 163–174.
[2] D. Kušščer, J. Holc, S. Hrovat, D. Kolar, Correlation between the defect structure, conductivity and chemical stability of $La_{1-y}Sr_yFe_{1-x}Al_xO_{3-\delta}$ cathodes for SOFC, J. Eur. Ceram. Soc. 21 (2001) 1817–1820.
[3] A. Mai, V.A.C. Haanappel, S. Uhlenbruck, F. Tietz, D. Stöver, Ferrite-based perovskites as cathode materials for anode-supported solid oxide fuel cells. Part I. Variation of composition, Solid State Ionics 176 (2005) 1341–1350.
[4] A. Mai, V.A.C. Haanappel, S. Uhlenbruck, F. Tietz, D. Stöver, Ferrite-based perovskites as cathode materials for anode-supported solid oxide fuel cells. Part II. Influence of the CGO interlayer, Solid State Ionics 177 (2006) 2103–2107.
[5] Y. Teraoka, H.M. Zhang, K. Okamoto, N. Yamazoe, Mixed ionic–electronic conductivity of $La_{1-x}Sr_xCo_{1-y}FeyO_{3-\delta}$ perovskite-type oxides, Mater. Res. Bull. 23 (1988) 51–58.
[6] J. Fleig, On the width of the electrochemically active region in mixed conducting solid oxide fuel cell cathodes, J. Power Sources 105 (2002) 228–238.
[7] V.A.C. Haanappel, J. Mertens, D. Rutenbeck, C. Tropartz, W. Herzhof, D. Sebold, F. Tietz, Optimisation of processing and microstructural parameters of LSM cathodes to improve the electrochemical performance of anode-supported SOFCs, J. Power Sources 141 (2005) 216–226.
[8] S.B. Adler, J.A. Lane, B.C.H. Steele, Electrode kinetics of porous mixed-conducting oxygen electrodes, J. Electrochem. Soc. 143 (1996) 3554–3564.
[9] J.A. Kilner, R.A. De Souza, I.C. Fullarton, Surface exchange of oxygen in mixed conducting perovskite oxides, Solid State Ionics 86–88 (1996) 703–709.
[10] J. Fleig, Solid oxide fuel cell cathodes: polarization mechanisms and modeling of the electrochemical performance, Annu. Rev. Mater. Res. 33 (2003) 361–382.
[11] V.V. Srdic, R.P. Omorjan, J. Seidel, Electrochemical performances of $(La,Sr)CoO_3$ cathode for zirconia-based solid oxide fuel cells, Mater. Sci. Eng. B 116 (2005) 119–124.
[12] E.P. Murray, M.J. Sever, S.A. Barnett, Electrochemical performance of $(La,Sr)(Co,Fe)O_3$–$(Ce,Gd)O_3$ composite cathodes, Solid State Ionics 148 (2002) 27–34.
[13] J.W. Kim, A.V. Virkar, K.Z. Fung, K. Mehta, S.C. Singhal, Polarization effects in intermediate temperature, anode-supported solid oxide fuel cells, J. Electrochem. Soc. 146 (1999) 69–78.
[14] Y. Leng, S. Chan, Q. Liu, Development of LSCF–GDC composite cathodes for low-temperature solid oxide fuel cells with thin film GDC electrolyte, Int. J. Hydrogen Energy 33 (2008) 3808–3817.
[15] N. Gunasekaran, S. Saddawi, J.J. Carberry, Effect of surface area on the oxidation of methane over solid oxide solution catalyst $La_{0.8}Sr_{0.2}MnO_3$, J. Catal. 159 (1996) 107–111.
[16] Y. Liu, H.T. Zheng, J.R. Liu, T. Zhang, Preparation of high surface area $La_{1-x}A_xMnO_3$ (A = Ba, Sr or Ca) ultra-fine particles used for CH_4 oxidation, Chem. Eng. J. 89 (2002) 213–221.
[17] M.J. Jorgensen, S. Primdahl, C. Bagger, M. Mogensen, Effect of sintering temperature on microstructure and performance of LSM–YSZ composite cathodes, Solid State Ionics 139 (2001) 1–11.
[18] A. Hagiwara, N. Hobara, K. Takizawa, K. Sato, H. Abe, M. Naito, Microstructure control of SOFC cathodes using the self-organizing behavior of LSM/ScSZ composite powder material prepared by spray pyrolysis, Solid State Ionics 178 (2007) 1123–1134.
[19] A. Dutta, J. Mukhopadhyay, R.N. Basu, Combustion synthesis and characterization of LSCF-based materials as cathode of intermediate temperature solid oxide fuel cells, J. Eur. Ceram. Soc. 29 (2009) 2003–2011.
[20] S. Shukla, S. Seal, R. Vij, S. Bandyopadhyay, Reduced activation energy for grain growth in nanocrystalline yttria-stabilized zirconia, Nano Lett. 3 (2003) 397–401.
[21] Q.S. Zhu, B.A. Fan, Low temperature sintering of 8YSZ electrolyte film for intermediate temperature solid oxide fuel cells, Solid State Ionics 176 (2005) 889–894.
[22] M.G. Bellino, D.G. Lamas, N.E.W. de Reca, Enhanced ionic conductivity in nanostructured, heavily doped ceria ceramics, Adv. Funct. Mater. 16 (2006) 107–113.
[23] H.S. Song, S. Lee, S.H. Hyun, J. Kim, J. Moon, Compositional influence of LSM–YSZ composite cathodes on improved performance and durability of solid oxide fuel cells, J. Power Sources 187 (2009) 25–31.
[24] H.S. Song, W.H. Kim, S.H. Hyun, J. Moon, Influences of starting particulate materials on microstructural evolution and electrochemical activity of LSM–YSZ composite cathode for SOFC, J. Electroceram. 17 (2006) 759–764.
[25] S. Lee, H.S. Song, S.H. Hyun, J. Kim, J. Moon, LSCF–SDC core–shell high-performance durable composite cathode, J. Power Sources 195 (2010) 118–123.
[26] M. Mamak, N. Coombs, G. Ozin, Electroactive mesoporous yttria stabilized zirconia containing platinum or nickel oxide nanoclusters: a new class of solid oxide fuel cell electrode materials, Adv. Funct. Mater. 11 (2001) 59–63.
[27] M. Shah, S.A. Barnett, Solid oxide fuel cell cathodes by infiltration of $La_{0.6}Sr_{0.4}Co_{0.2}Fe_{0.8}O_{3-\delta}$ into Gd-doped ceria, Solid State Ionics 179 (2008) 2059–2064.